Sensors & Transducers, Vol. 231, Issue 3, March 2019, pp. 25-30

www.sensorsportal.com

Sensors & Transducers

Published by IFSA Publishing, S. L., 2019
http://www.sensorsportal.com

Modeling and Simulation of Low-Cost and Low-Magnetic Field Magnetic Resonance Imaging

Sweta GHOSH, Prateek Kumar SONKER and * Shubhajit Roy CHOWDHURY
School of Computing and Electrical Engineering
IIT Mandi, Kamand – 175005, Mandi, H. P., India
* Tel.: +91 1905 267110, fax: +91 1905 267009
E-mail: src@iitmandi.ac.in

Received: 3 March 2019 /Accepted: 27 March 2019 /Published: 29 March 2019

Abstract: Magnetic Resonance Imaging as the name suggests is a technique of obtaining image using magnetic field and resonance of the nucleus. The study done in this paper aims to propose a design and model a low magnetic field Magnetic resonance imaging in which Helmholtz coil plays a vital part. Commercially available machines generally use permanent magnet or superconducting magnet. This magnet has been replaced with Helmholtz coil in the design proposed in this paper. The Helmholtz coil produces a magnetic field of 0.2 T which is also homogenous upto ±2 percent in the region of study. This homogeneity inspired to go for this design. Along with the Helmholtz coil, other necessary coils are gradient coils and radio-frequency coil. Maxwell and Saddle coils are used as gradient coils having a gradient strength of 75 μT/m. The resonating frequency for this magnetic field is 8.526 MHz. A prototype of this machine with scaled low magnetic field is under development.

Keywords: Helmholtz coil, Maxwell coil, Radio-frequency coil, Homogeneity, Saddle coil, Resonant frequency.

1. Introduction

Magnetic resonance imaging (MRI) is a non-invasive method of imaging of soft tissues and organs. MRI basically uses a variety of magnetic fields to produce an image. These fields are created by magnets and coils. Mostly permanent magnet or superconducting magnet is used to serve the purpose.

Magnetic resonance imaging as the name suggests uses the principle of nuclear alignment due to the magnetic field and resonance of the nucleus present in the biological bodies to obtain an image. Basically the hydrogen ions (protons) that are within the field are affected due to the magnetic field. The magnetic field aligns the nucleus in a single direction. Gradients play an important role in spatial and temporal encoding. They further change the nuclear alignment in a specific way. Then after when resonance frequency is applied the nucleus emits certain signals that are obtained as MR signals.

Magnetic resonance imaging was established in early 1980's. There are high magnetic field as well as low magnetic field MRI's. For both the cases the image formation depends upon the signal-to-noise ratio (SNR). Higher the SNR, better is the image quality. High magnetic field MRI produces high SNR, good contrast and resolution compared to low magnetic field MRI. While high magnetic field (≥ 1.0 T) MRI scanners continue to be the most commonly used, there is growing interest in the utilization of low-field (≤ 0.5 T) extremity scanners [6]. They are smaller, less expensive, and easier to install, and allow for quicker patient diagnoses in an office setting. It is possible for low-field scanners to

improve image quality by increasing scan duration, although doing so also increases the chance of motion artifacts [1-4]. While low field MRI images may not be able to compete with the quality of those produced using high-field scanners, it is important to consider whether or not they can provide comparable diagnostic capabilities to justify their logistical benefits. When compared with surgical findings, the use of low-field extremity MRI scanners for identifying medial meniscus pathology has been promising (sensitivity, 77 %-96 %; specificity, 71 %-100 %); however, results for identifying pathology of the lateral meniscus have been more variable [5-13]. Most of these studies show low-field MRI to be a moderately good identifier of sub-peripheral and meniscus pathology (sensitivity, 75 %-93 %; specificity, 94 %-100 %).

Ghazinoor and Crues, *et al*., concluded that their subjective experience is in concordance with many studies demonstrating the high diagnostic value in the use of low-field scanners in musculoskeletal pathology [1].

Tavernier and Cotton, *et al*., stated that the primary limitation of low-field MRI is lower SNR, which has to be compensated for by increasing the slice thickness, reducing the in-plane resolution, increasing the number of acquisitions (and consecutively the acquisition time), and decreasing the bandwidth [14].

Tavernier and Cotton, *et al*., concluded that implementation of low-field MRI systems may be useful, especially in orthopaedic centres, or if installation of an additional high-field scanner is not possible because of economic considerations [14]. Blanco, *et al*., showed that there is trade-off in image quality towards less resolution due to open structure of these systems [15]. In a review article, Hayashi, *et al*., noted that no reliable efficacy studies, however, exist comparing the diagnostic capabilities of low-versus high-field scanners [16]. In order to compensate for lower SNR, scanners with low field strength tend to have longer acquisition times, often resulting in greater image degradation due to patient movement. However, it is widely accepted that today's low-field scanners provide sufficient diagnostic information when spin-echo and gradient-echo techniques are used. Hayashi, *et al*., conclude recent technological developments in the realm of low-field MR scanners will lead to higher image quality, shorter scan times, and refined imaging protocols [16]. Utilization of low-field systems has the potential to enhance overall cost reductions with little or no loss of diagnostic performance.

There are numerous, very small, comparative studies that validate low-field MRI is superior to x-ray in the detection of rheumatoid arthritis (RA) findings (e.g., bone erosion, joint-space narrowing, synovitis); [16-20]. A few small, comparative studies have evaluated the diagnostic capability of low-field MR with conventional MR in the detection of RA findings. Using conventional MRI as the standard reference, Ejbjerg, *et al*., evaluated findings from a 0.2 T extremity dedicated MR scanner in thirty seven patients with RA. Low field MR (3D gradient echo sequence) wrist and metacarpophalangeal (MCP) joint imaging demonstrated sensitivity, specificity, and accuracy for erosions of 94 %, 93 %, 94 %; for synovitis, 90 %, 96 % and 94 %; and for bone marrow edema, 39 %, 99 %, and 95 % [20]. The authors stated that low-field extremity-dedicated MRI provides similar information on bone erosions and synovitis as high-field MRI units.

The current research focuses on the development of the low cost and low magnetic field MRI machine for the point of ease testing support. In order to provide the diagnostics support at the point of care, the MRI has been proposed to have sufficient small weight, because of which Helmholtz coil instead of permanent magnetic is proposed to be used to generate the main magnetic field. The current work proposes to use 0.2 T magnetic field for generating the MR image. The gradient coil is implemented with Maxwell coil and Saddle coil.

The RF coil design has been implemented using spiral coil. Based on the procedure used by Mehmet Bilgen in 2004 and 2001 [21-22] in which their study showed implantable coils can work well having good SNR. Further study revealed simple spiral coils can work well as transmitter and receiver [23]. A simple spiral coil has been used as the RF coil.

This paper is aimed to design and model a low magnetic field MRI. Material and method and design and modelling of the MRI system are depicted in the following sections. Results are also discussed.

2. Materials and Methods

The proposed design of MRI is based on Helmholtz Coil. The different coils that are used to build the coil are Helmholtz coil in place of permanent magnet, Maxwell coil and Saddle coils as the gradient coils and lastly radio-frequency (RF) coils. Helmholtz Coil is used for generating the main magnetic field of 0.2 T. The gradient strength has been kept at 75 μT/m which is necessary for obtaining temporal and spatial information. All these coils are concentric in nature. The inner radius of the system is 40 cm, which is enough for head or limbs to be inserted. All the coils are built with annealed copper on a wooden base material. For the coils, copper wires are used with AWG gauge size of 11 (2.303 mm diameter). For RF coil, very thin copper wire was used of gauge size 20.

3. Design and Modeling of Coils

3.1. Helmholtz Coil

The governing principle of Helmholtz coil is based on the Biot Savart's law. The Biot Savarts law is given in Eq. (1). A little modification in this law. yields the formula for the above mentioned coil. According to the geometry of the Helmholtz coil the magnetic field

is given in Eq. (2). Eq. (2) describes the magnetic field at a point halfway between the coils.

$$\boldsymbol{B_1(x)} = \frac{\boldsymbol{\mu_0 InR^2}}{\boldsymbol{2(R^2 + x^2)^{3/2}}}, \quad (1)$$

$$B_1\left(\frac{R}{2}\right) = \left(\frac{8}{5\sqrt{5}}\right)\frac{\mu_0 nI}{R}, \quad (2)$$

where μ_0 is the permeability constant = $4\pi \times 10^{-7}$ Tm/A;

I is the current in the coil;

R is the radius of the coil;

x is the distance of a point from the coil on the axis of the coil;

n is the number of turns of the coil;

$\boldsymbol{B_1(x)}$ is the magnetic field generated along the axis of the coil due to current I.

For a current of 10 A and a number of turns 6675 in each coil, with a radius of 30 cm, a magnetic field of 0.2 T was obtained at the center of the coil. Homogeneity is calculated from the center of the coil to any particular point and it is measured in percentage change of magnetic field strength from center to any particular point.

$$H(\%) = \frac{B_i - B_0}{B_0} \times 100 \quad (3)$$

H is the homogeneity or percentage change of magnetic field strength at any point from the center. B_i is the magnetic field at any point in the volume and B_0 is the magnetic field at the center. The geometry of the coil is shown in Fig. 1.

Fig. 2 shows a pair of Helmholtz coil.

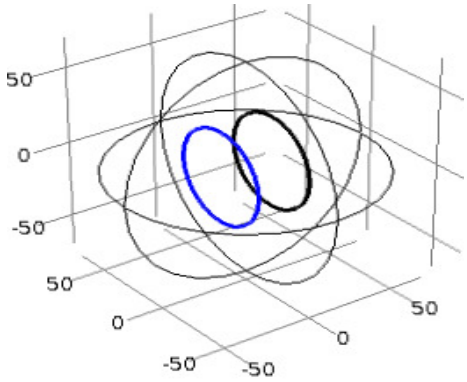

Fig. 1. Geometry of Helmholtz coil pair of radius 30 cm.

3.2. Gradient Coils

Gradient coils are an important part in the MRI system. These coils actually help in producing image. Maxwell coil and Saddle coils are used as gradient coils. The geometry of the Maxwell coil and Saddle coil are such that it not only generates the desired magnetic flux but also its orientation helps to enter the subject without any obstacle. This would not have been possible if all gradient coils were Maxwell coils.

Fig. 2. Helmholtz coil.

A gradient strength of 75 μT/m is used. These coils frequency encode the spatial information of the signal returned by the subject. The basic equation governing the linearly varying the gradient magnetic field is given by Eq. (4).

$$B_z(x,y,z) = B_0 + \frac{\partial B_z}{\partial x}x + \frac{\partial B_z}{\partial y}y + \frac{\partial B_z}{\partial z}z = B_0 + G_x x + G_y y + G_z z \quad (4)$$

B_0 is the main magnetic field. G_x and G_y are the transverse gradient and G_z is the longitudinal gradient. The Maxwell coil magnetic field is given by Eq. (5) whereas the Saddle coil equation is given in Eq. (6). Fig. 3 shows orientation of magnetic lines of force of Maxwell coil and Fig. 4 shows a gradient coil.

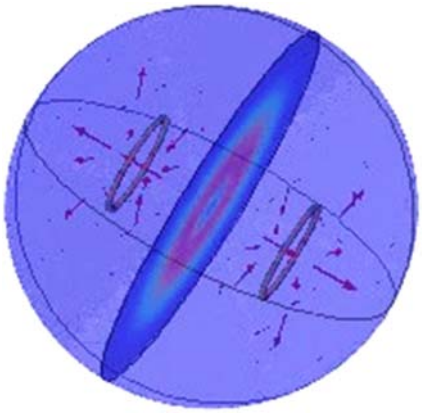

Fig. 3. Maxwell coil and magnetic lines of force.

Fig. 4. Gradient Coil.

$$B_Z = \frac{\mu_0 I a^2}{2\left[\left(d/2 - z\right)^2 + a^2\right]^{3/2}} - \frac{\mu_0 I a^2}{2\left[\left(d/2 + z\right)^2 + a^2\right]^{3/2}}, \quad (5)$$

$$B_z(y,z) = \frac{\mu_0 I}{2\pi} \frac{b-y}{(b-y)^2 + (d-z)^2} \quad (6)$$

In case of Maxwell coil (Eq. (5)); B_z is the magnetic field along the z axis due to the current in the coils. μ_0 is the permeability constant, I is the current in coil (in Amperes), a is the radius of coil (in meters) and z and d are the distance of a point from the coil on the axis (in meters) and the distance between the coils respectively.

Regarding the magnetic field produced by Saddle coils (Eq. (6)), B_z represents the gradient field along y direction and b and d are the co-ordinates in the yz plane. For x direction the Saddle coil is rotated 90°.

3.3. Radio-frequency Coil

The RF coil consists of a transmitter and receiver section. The transmitter section radiates the sample with a RF field in order to tip the magnetisation away from equillibrium position and that it can generate a detectatble NMR signal. The receiver section receives the signal and transforms the signal from analog to digital using some necessary circuitry.

The protons in the subject or patients go from one energy state to another energy state by releasing energy. That is they emit photon of some frequency to move from an excited state to equilibrium state. This frequency is directly proportional to the magnetic field strength. The relation between the resonating frequency and the main magnetic field is given by Eq. (7).

$$\omega = \gamma B_0, \quad (7)$$

where ω is the angular frequency. B_0 is the main magnetic field and γ is the gyromagnetic ratio for protons whose value is 42.58 MHz/T. From the fact that main magnetic field is 0.2 T the resonating frequency comes out to be 8.526 MHz. This frequency is also called the Larmor frequency of the nucleus.

The receiver and transmitter section are both spiral coil having small diameter. Both have the same resonating frequency of 8.526 MHz. For better SNR, the transmitter and the receiver are placed very close to the subject. For the encoder IC a 750 kΩ resistor and a 33 kΩ resistor are connected between the oscillator pins of decoder IC. Coiling was done with copper wires having AWG gauge size 20 that can resist a maximum current of 5 A.

4. Results

4.1. Simulation of Helmholtz Coil

The model of Helmholtz Coil has been built in COMSOL Multiphysics. The coil was designed for a magnetic field strength of 0.2 T. The inner radius of the coil has been kept 30 cm while the outer radius extends up to 59 cm. Copper was chosen as the base material for coiling. Using the equation of the magnetic field the number of turns obtained was 6675 for a current of 10 A. Having considered these specifications the magnetic flux density was obtained from the simulation shown in Fig. 5.

The uniformity of the coil can be observed from the figure. Also a line graph has been obtained from the simulation shown in Fig. 6.

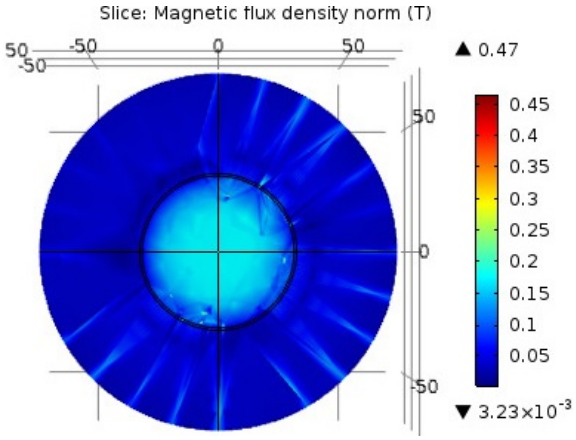

Fig. 5. Magnetic flux density distribution.

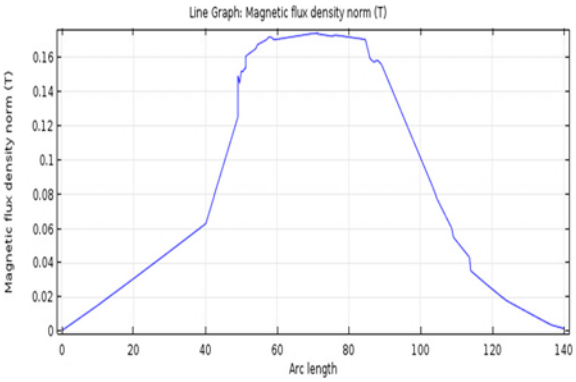

Fig. 6. Homogeneity of Helmholtz coil after simulation.

4.2. Simulation of Maxwell Coil

Maxwell Coil is anti-Helmholtz coil and has been used for longitudinal gradient and Saddle coil has been used for transverse gradient. In Maxwell coil the distance between the coils is √3 times the radius of the coil. The radius of the coil has been taken as 25 cm and the current 5 A. Having these specifications the number of turns obtained was 125 and the slope or

gradient strength was 75 μT/m. The slope was determined from the graph in Fig. 7.

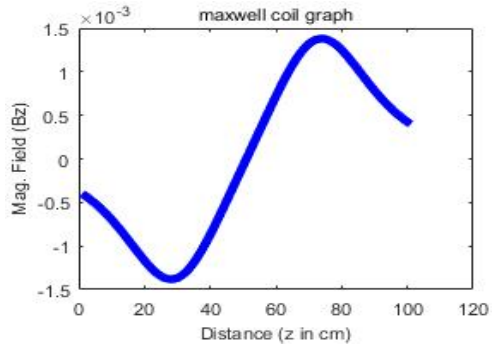

Fig. 7. Slope of Maxwell coil.

The simulation result shows the distribution of magnetic flux density of the Maxwell coil (Fig. 8). From the figure it can be clearly seen that the magnetic flux density increases from the center to outwards. This assures that a gradient slope can be obtained from the coil. Also the slope can be chosen desirably. Fig. 8 shows the flux distribution.

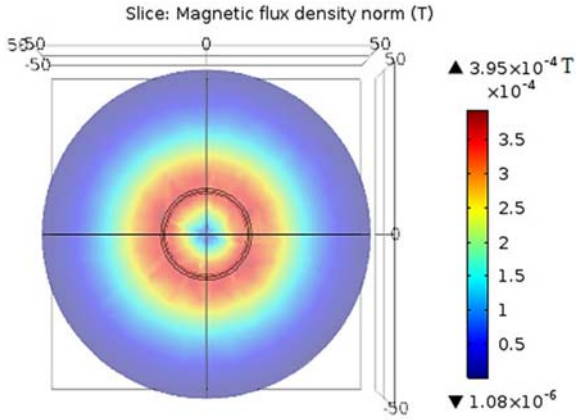

Fig. 8. Magnetic flux density distribution of Maxwell coil.

4.3. RF Coil

The RF coil consists of two parts, the transmitter part and the receiver part. Both these parts are designed separately. The design of the transmitter part and receiver part are both spiral coils. From the transmitter section the output signal can be directly viewed in the oscilloscope. The RF coil was implemented as shown in Fig. 9.

5. Discussion

Simulation studies of the Helmholtz coil and the Maxwell coil shows the distribution of magnetic flux density of the coils. Regarding the Helmholtz coil the flux density was found to be 0.2 T (calculated and simulated). For the Maxwell coil, the flux density is zero at the center of the coil, which is also depicted by the simulation result. From the flux density graph in figure and the homogeneity graph in figure it can clearly be inferred that the field is homogeneous within the coil. The flux density is constant within some region of the coil (region of study) inferring that field is homogenous in that region.

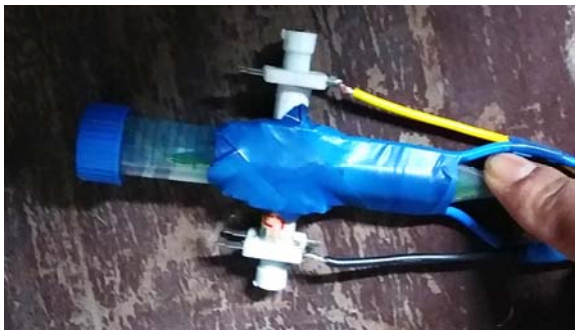

Fig. 9. The transmitter and receiver of RF coil.

A study of homogeneity along the radial length of the coil is given in Table 1. And it can be seen that homogeneity lies within ±2 % in the region of study.

The RF coil is spiral and has been made such that it can be placed very close to the subject for a better received signal. Both the transmitter and receiver work at the same resonating frequency which is 8.526 MHz.

Table 1. Homogeneity obtained from simulation of Helmholtz coil.

Radius (cm)	Homogeneity (%)
4.29	0.33
11.5	0.48
11.85	0.47
12.9	1.8
14.53	2.63
25.85	39

6. Conclusion

This paper presents a design of Helmholtz coil, Gradient coil and RF coil for the development of a low cost and low magnetic field MRI system. The simulation results have been obtained for Helmholtz coil and Maxwell coil in z-direction for magnetic flux density, magnetic field at the centre of the coil and over the surface of the coils obtained from COMSOL Multiphysics 5.2. The plots obtained from the COMSOL and our calculated data shows the exact same values prove that our approach is accurate. This study reveals that there occurs homogeneity in Helmholtz coil where the subject can be placed for study. Calculated values were validated through simulation that homogeneity at the centre of Helmholtz coil is about ±2 per cent over the region of study. The RF receiver and transmitter was spiral in nature and received the output signals that were observed in oscilloscope. A prototype of 0.2 T MRI is under development with scaled down magnetic field.

This machine will be useful and harmless for mankind and will give the better results as compared to bulky machines.

References

[1]. S. Ghazinoor, J. V. Crues, Low field MRI: a review of the literature and our experience in upper extremity imaging, *Clinics in Sports Medicine*, Vol. 25, Issue 3, 2006, pp. 591–606.

[2]. S. Ghazinoor, J. V. Crues, C. Crowley, Low-field musculoskeletal MRI, *Journal of Magnetic Resonance Imaging*, Vol. 25, Issue 2, 2007, pp. 234–244.

[3]. R. Loew, K. Kreitner, M. Runkel, J. Zoellner, M. Thelen, MR arthrography of the shoulder: comparison of low-field (0,2 T) vs high-field (1.5 T) imaging, *European Radiology*, Vol. 10, Issue 6, 2000, pp. 989–996.

[4]. K. Woertler, M. Strothmann, B. Tombach, P. Reimer, Detection of articular cartilage lesions: Experimental evaluation of low- and high-field-strength MR imaging at 0.18 and 1.0 T, *Journal of Magnetic Resonance Imaging*, Vol. 11, Issue 6, 2000, pp. 678–685.

[5]. M. J. Barnett, MR diagnosis of internal derangements of the knee: effect of field strength on efficacy, *American Journal of Roentgenology*, Vol. 161, Issue 1, 1993, pp. 115–118.

[6]. A. Cotten, E. Delfaut, X. Demondion, F. Lap`egue, M. Boukhelifa, N. Boutry, P. Chastanet, F. Gougeon, MR imaging of the knee at 0.2 and 1.5 T: correlation with surgery, *American Journal of Roentgenology*, Vol. 174, Issue 4, 2000, pp. 1093–1097.

[7]. Fischer S. P., W. Del Pizzo, Friedman M. J., *et al*., Accuracy of diagnoses from magnetic resonance imaging of the knee, *J Bone Joint Surg Am*., 73, 1, 1991, pp. 2-10.

[8]. J. L. Glashow, R. Katz, M. Schneider, W. Scott, Double-blind assessment of the value of magnetic resonance imaging in the diagnosis of anterior cruciate and meniscal lesions, *J Bone Joint Surg Am*, Vol. 71, Issue 1, 1989, pp. 113–119.

[9]. J. Kinnunen, S. Bondestam, A. Kivioja, J. Ahovuo, S. K. Toivakka, I. Tulikoura, T. Karjalainen, Diagnostic performance of low field MRI in acute knee injuries, *Magnetic Resonance Imaging*, Vol. 12, Issue 8, 1994, pp. 1155–1160.

[10]. H. S. Lokannavar, X. Yang, H. Guduru, Arthroscopic and low-field MRI (0.25 T) evaluation of meniscus and ligaments of painful knee, *Journal of Clinical Imaging Science*, Vol. 2, 2012.

[11]. B. R. Mandelbaum, G. A. Finerman, M. A. Reicher, S. Hartzman, L. W. Bassett, R. H. Gold, W. Rauschning, F. Dorey, Magnetic resonance imaging as a tool for evaluation of traumatic knee injuries. Anatomical and pathoanatomical correlations, *The American Journal of Sports Medicine*, Vol. 14, Issue 5, 1986, pp. 361–370.

[12]. K.-A. Riel, M. Reinisch, B. Kersting-Sommerhoff, N. Hof, T. Merl, 0.2-Tesla magnetic resonance imaging of internal lesions of the knee joint: a prospective arthroscopically controlled clinical study, *Knee Surgery, Sports Traumatology, Arthroscopy*, Vol. 7, Issue 1, 1999, pp. 37–41.

[13]. R. T. Blanco, R. Ojala, J. Kariniemi, J. Per¨al¨a, J. Niinim¨aki, O. Tervonen, Interventional and intraoperative MRI at low field scanner– a review, *European Journal of Radiology*, Vol. 56, Issue 2, 2005, pp. 130-142.

[14]. T. Tavernier, A. Cotten, High-versus low-field mr imaging, *Radiologic Clinics of North America*, Vol. 43, Issue 4, 2005, pp. 673–681.

[15]. N. Hayashi, Y. Watanabe, T. Masumoto, H. Mori, S. Aoki, K. Ohtomo, O. Okitsu, T. Takahashi, Utilization of low-field MR scanners, *Magnetic Resonance in Medical Sciences*, Vol. 3, Issue 1, 2004, pp. 27–38.

[16]. H. Yoshioka, S. Ito, S. Handa, S. Tomiha, K. Kose, T. Haishi, A. Tsutsumi, T. Sumida, Low-field compact magnetic resonance imaging system for the hand and wrist in rheumatoid arthritis, *Journal of Magnetic Resonance Imaging*, Vol. 23, Issue 3, 2006, pp. 370–376.

[17]. A. K. Scheel, K. A. Hermann, S. Ohrndorf, C. Werner, C. Schirmer, J. Detert, M. Bollow, B. Hamm, G. A. M¨uller, G. R. Burmester, *et al*., Prospective 7 year follow up imaging study comparing radiography, ultrasonography, and magnetic resonance imaging in rheumatoid arthritis finger joints, *Annals of the Rheumatic Diseases*, Vol. 65, Issue 5, 2006, pp. 595– 600.

[18]. B. Ejbjerg, E. Narvestad, M. Szkudlarek, J. Jacobsen, H. Thomsen, M. Ostergaard, Optimized, low-cost, low-field dedicated extremity MRI can provide similar information on wrist and mcp joint synovitis and bone erosions as expensive conventional high-field MRI arthritis-a comparison with 'conventional' high-field MRI, Conference Poster, *Ann Rheum* Dis, 2002.

[19]. J. V. Crues, F. G. Shellock, S. Dardashti, T. W. James, O. M. Troum, Identification of wrist and metacarpophalangeal joint erosions using a portable magnetic resonance imaging system compared to conventional radiographs, *The Journal of Rheumatology*, Vol. 31, Issue 4, 2004, pp. 676–685.

[20]. H. Lindegaard, J. Vallo, K. Hørslev-Petersen, P. Junker, M. Ostergaard, Low field dedicated magnetic resonance imaging in untreated rheumatoid arthritis of recent onset, *Annals of the Rheumatic Diseases*, Vol. 60, Issue 8, 2001, pp. 770–776.

[21]. M. Bilgen, Simple low cost multipurpose RF coil for MR microscopy at 9.4 T, *Magnetic Resonance in Medicine*, Vol, 52, 2004, pp. 937–940.

[22]. M. Belgen, I. Elshafiey, P. A. Narayana, In vivo magnetic resonance microscopy of rat spinal cord at 7 T using implantable RF coils, *Magnetic Resonance in Medicine*, Vol. 46, Issue 6, 2001, pp. 1250–1253.

[23]. O. Aghogho, A method of moments approach for the design of RF coils for MRI, *Worcester Polytechnic Institute,* March 2008.